MOLECULAR AND CELLULAR BIOLOGY, Mar. 2007, p. 2202–2214 Vol. 27, No. 6
0270-7306/07/$08.00+0 doi:10.1128/MCB.01908-06

Crucial Role of *Bysl* in Mammalian Preimplantation Development as an Integral Factor for 40S Ribosome Biogenesis▽†

Kenjiro Adachi,[1] Chie Soeta-Saneyoshi,[1]‡ Hiroshi Sagara,[2] and Yoichiro Iwakura[1]*

Center for Experimental Medicine[1] and Fine Morphology Laboratory,[2] Institute of Medical Science, University of Tokyo, Minato-ku, Tokyo, Japan

Received 9 October 2006/Returned for modification 15 November 2006/Accepted 4 January 2007

Blastocyst formation during mammalian preimplantation development is a unique developmental process that involves lineage segregation between the inner cell mass and the trophectoderm. To elucidate the molecular mechanisms underlying blastocyst formation, we have functionally screened a subset of preimplantation embryo-associated transcripts by using small interfering RNA (siRNA) and identified *Bysl* (bystin-like) as an essential gene for this process. The development of embryos injected with *Bysl* siRNA was arrested just prior to blastocyst formation, resulting in a defect in trophectoderm differentiation. Silencing of *Bysl* by using an episomal short hairpin RNA expression vector inhibited proliferation of embryonic stem cells. Exogenously expressed Bysl tagged with a fluorescent protein was concentrated in the nucleolus with a diffuse nucleoplasmic distribution. Furthermore, the loss of *Bysl* function by using RNA interference or dominant negative mutants caused defects in 40S ribosomal subunit biogenesis. These findings provide evidence for a crucial role of Bysl as an integral factor for ribosome biogenesis and suggest a critical dependence of blastocyst formation on active translation machinery.

Blastocyst formation is the first differentiation process during mammalian embryonic development, leading to the segregation of two distinct cell lineages: the inner cell mass (ICM) and the trophectoderm (TE) (27). Prior to blastocyst formation, intercellular junctions are established during compaction and cellular polarity is developed. The subsequent rounds of asymmetric divisions give rise to spatially segregated outer and inner cells. The outer layer of cells adopts a polarized epithelial structure differentiating into the TE, which then contributes to extraembryonic tissues, including the placenta. The apolar ICM is the founder cell population of the embryo proper. The ICM and its successor, the epiblast, comprise transient pluripotent stem cell populations. After implantation, the cells begin to differentiate into specific cell types that will form the three primary germ layers. Embryonic stem (ES) cells, which are derived from the ICM or epiblast, self-renew and maintain pluripotent differentiation capacity in culture. Although the regulatory networks that are responsible for the maintenance of ES cell identity have been extensively investigated, molecular analysis of preimplantation development is quite limited due to the scarcity of materials and experimental approaches.

With the advent of the genome projects, global gene expression profiles of various tissues and developmental stages have been generated from cDNA libraries and microarray analyses. These studies have provided an effective way to identify genes that are preferentially expressed in specific cell types or tissues, especially in early embryos from which only small amounts of material can be obtained. In addition, gene silencing by RNA interference (RNAi) has been established as a method for reverse genetic analysis of gene function in mammalian cells, allowing a time- and cost-effective comprehensive approach. Particularly in preimplantation embryos, loss-of-function analysis using RNAi has a great advantage over gene disruption in that it can eliminate the expression of maternal transcripts (69).

To elucidate the molecular mechanisms that control blastocyst formation, we took advantage of in silico expression analysis combined with RNAi. Using database mining, we identified several genes whose expression is enriched in preimplantation embryos. These were then functionally screened using small interfering RNA (siRNA) to identify genes important for preimplantation development. Among them, siRNA against *Bysl* (bystin-like) most significantly inhibited blastocyst formation when it was microinjected into fertilized eggs. We also found that knockdown of *Bysl* inhibited proliferation of ES cells.

Mammalian *Bysl* was first identified as a cytoplasmic component of a complex that mediates homophilic cell adhesion between human trophoblast and endometrial epithelial cells in vitro (62). In an expression assay, a cDNA encoding human BYSL was found to facilitate the adhesion of cells that express the integral membrane protein TRO (trophinin) to endometrial adenocarcinoma cells. In this context, BYSL could interact directly with TRO and the cytoplasmic protein TROAP (trophinin-associated protein). Immunocytochemical analysis showed that BYSL localized in the cytoplasm of trophoblastic teratocarcinoma cells (62). They are coexpressed in the trophoblast and endometrial epithelial cells at the utero-placental interface only around the time of implantation (61). These studies suggested that a TRO-TROAP-BYSL complex might be involved in the attachment process at implantation.

* Corresponding author. Mailing address: Institute of Medical Science, University of Tokyo, 4-6-1 Shirokanedai, Minato-ku, Toyko 108-8639, Japan. Phone: 81-3-5449-5536. Fax: 81-3-5449-5430. E-mail: iwakura@ims.u-tokyo.ac.jp.

† Supplemental material for this article may be found at http://mcb.asm.org/.

‡ Present address: Oregon Health and Science University, Portland, OR.

▽ Published ahead of print on 22 January 2007.

The functional significance of *Bysl* in the developmental context has been demonstrated in mice. *Bysl* is expressed in the epiblast of embryonic day 5.5 (E5.5) mouse embryos, and *Bysl*-deficient mice show embryonic lethality shortly after implantation (5, 38). These results indicate that *Bysl* is not required for the implantation process, as had been suggested by the earlier studies (61, 62). Thus, the functional roles of mammalian *Bysl* in early embryonic development are controversial and remain to be elucidated.

Bysl is highly conserved from yeasts to humans (11, 51). The yeast *Saccharomyces cerevisiae* homolog of Bysl, Enp1, localizes to the nucleus and accumulates in the nucleolus with only a weak cytoplasmic distribution and is essential for 40S ribosome biogenesis (11, 54). A temperature-sensitive mutant of *ENP1* is defective in the early steps of rRNA processing and in the nuclear export of pre-40S subunits. *Caenorhabditis elegans byn-1* is expressed in germ line cells, embryos, and larvae. Systematic functional analysis using RNAi showed that *byn-1* plays an essential role in both germ lines and embryonic tissues (28). *Drosophila melanogaster bys* is predominantly expressed in the ovarian nurse cells and in embryonic and larval tissues undergoing morphogenetic processes, suggesting a role in cell growth (58). Bys in this organism was shown to localize also to the nucleus. Thus, currently available data suggest that the roles of mammalian *Bysl* and its homologs in lower organisms are quite different.

In this study, we investigated the role of mouse *Bysl* in early embryonic development. Exogenously expressed Bysl tagged with a fluorescent protein localized to the nucleus with enrichment in the nucleolus. Furthermore, the loss of *Bysl* function using RNAi or dominant negative mutants caused defects in 40S ribosomal subunit biogenesis. These findings provide evidence for the essential role of *Bysl* in early embryonic development and suggest a critical dependence of blastocyst formation on the activation of translation machinery.

MATERIALS AND METHODS

Microinjection of siRNAs into mouse embryos. siRNA duplexes of 21 nucleotides against the following target sequences were in vitro transcribed with a *CUGA7* in vitro siRNA synthesis kit (Nippon Genetech, Japan): siEGFP-441, CAGCCACAACGUCUAUAUCAU (66); siOct3/4-670, AAGAGAAAGCGAACUAGCAUU (66); siBysl-773, GAGAUGACAUUGCUGAAUACA; siBysl-845, CUGGAGCCUGGUUCAAAGGAA; and siBysl-976, CUGAAGAUCGCAGAAAUGGAA. The siRNA number represents the nucleotide position within the coding region that corresponds to the 3′ end of the siRNA antisense strand. Transcribed siRNAs were purified and resuspended in RNase-free water. Microinjection was performed under an inverted microscope using a programmable pneumatic microinjector (IM-300; Narishige). At E0.5 (24 h after hCG administration), fertilized eggs from BDF1 × BDF1 mating were injected with a few picoliters of 20 μM siRNA duplexes and cultured in M16 medium (Sigma).

RT-PCR analysis. Total RNA was isolated with Sepasol RNA I Super reagent (Nacalai Tesque, Kyoto, Japan). First-strand cDNA was synthesized from total RNA with SuperScript III reverse transcriptase (Invitrogen). The following primers were used for RT-PCR: *Bysl*-F (AGGAGTCCGGGAGGTGTTAT), *Bysl*-R (GCCAGAAAGTGGAAGACCAG), *Oct3/4*-F (GGCGTTCTCTTTGGAAAGGT), *Oct3/4*-R (CTCGAACCACATCCTTCTCT), *Cdx2*-F (ACATCACCATCAGGAGGAAAAG), *Cdx2*-R (CACTGGGTGACAGTGGAGTTTA), *EndoA*-F (GGCAGATCCATGAAGAGGAG), *EndoA*-R (CTTGCGGTAGGTGGTGATCT), *Nanog*-F (AGGGTCTGCTACTGAGATGC), *Nanog*-R (CAACCACTGGTTTTTCTGCC), *Rex1*-F (CAATAGAGTGAGTGTGCAGTGC), *Rex1*-R (CCTCTGTCTTCTCTTGCTTCG), *Hnf4*α-F (TGCCCTCTCACCTCAGCAATG), *Hnf4*α-R (CCCCTCAGCACACGGTTTTG), *brachyury*-F (GTCTTCTGGTTCTCCGATGT), *brachyury*-R (CCAGGTGCTATATATTGCCT), *Gapdh*-F (GTGTTCCTACCCCCAATGTG), *Gapdh*-R (GTCATTGAGAGCAATGCCAG), β*actin*-F (AAGTGTGACGTTGACATCCG), and β*actin*-R (GATCCACATCTGCTGGAAGG) (F indicates the forward primer, and R indicates the reverse primer).

BrdU incorporation assay. Embryos were cultured in M16 medium supplemented with 10 μM 5-bromo-2′-deoxyuridine (BrdU) for 60 min to label dividing cells. The embryos were then fixed with 4% paraformaldehyde in phosphate-buffered saline (PBS), and DNA was denatured by incubation in 2 N HCl containing 0.2% Triton X-100 for 60 min at 37°C. After neutralization with 0.1 M sodium borate (pH 8.5), the embryos were blocked with 10% normal goat serum in PBS. BrdU incorporation was detected by incubation with mouse monoclonal anti-BrdU antibody (2 μg/ml; Roche) in PBS containing 1% bovine serum albumin at 4°C overnight, followed by Alexa Fluor 488-conjugated goat anti-mouse immunoglobulin G antibody.

Immunofluorescence analysis. For immunofluorescence staining, embryos were fixed with 4% paraformaldehyde in PBS and permeabilized in 0.2% Triton X-100 in PBS. After blocking with 10% normal goat serum in PBS, the embryos were incubated overnight at 4°C with the following antibodies in PBS containing 1% bovine serum albumin: rat monoclonal anti-cytokeratin 8 or EndoA (TROMA-1; Developmental Studies Hybridoma Bank) at 1:100, rabbit anti-Oct3/4 antiserum (44) at 1:10,000, and mouse monoclonal anti-Cdx2 (CDX2-88; BioGenex, CA) at the concentration given by the manufacturer. The embryos were then incubated for 30 min with Alexa Fluor 488- or 546-conjugated goat secondary antibodies against rat, rabbit, or mouse immunoglobulin at a dilution of 1:1,000. For nuclear staining, the embryos were incubated with 10 μg/ml Hoechst 33342 (Sigma) for 5 min and then observed under a confocal laser scanning microscope (Radiance 2100; Bio-Rad). For immunofluorescence staining of fibrillarin, mouse monoclonal anti-fibrillarin (38F3; Abcam) was used at 1:500, followed by Alexa Fluor 546-conjugated secondary antibody.

Plasmid construction. For episomal short hairpin RNA (shRNA) expression vectors, a human U6 promoter was amplified by PCR from pENTR/U6 (Invitrogen) with the following primers containing BbsI and AflIII sites for cloning of shRNA template oligonucleotides into the immediate downstream of the transcriptional initiation site: TACCAAGGTCGGGCAGGAAGAGGG (forward) and ACATGTGAAGACACGGGTGTTTCGTCCTTTCCACAAG (reverse) (the U6 promoter sequences are underlined). This U6 cassette was ligated to a PstI-EcoRV fragment of pHPCAG (42) harboring a polyoma origin of replication with a mutated enhancer, which enables the episomal maintenance of the plasmid, and a PGK-pac-pA cassette, generating pPPU6. For each shRNA expression construct, both top and bottom template oligonucleotides were annealed and ligated into BbsI/AflIII-digested pPPU6. The following shRNA template oligonucleotides were used: shEGFP-441 Top, caccgCAGTCACAATGTCTATGTCATgtgtgctgtccATGATATAGACGTTGTGGCTGttttt; shEGFP-441 Bottom, catgaaaaaCAGCCACAACGTCTATATCATggacagcacacATGACATAGACATTGTGACTGc; shBysl-845 Top, caccgCTGGAGCTTGGTTCGAGGAAgtgtgctgtccTTCCTTTGAACCAGGCTCCAGttttt; shBysl-845 Bottom, catgaaaaaCTGGAGCCTGGTTCAAAGGAAggacagcacacTTCCCTCGAACCAAGCTCCAGc; shBysl-976 Top, caccgCTGAGGATCGTAGAGATGGAAgtgtgctgtccTTCCATTTCTGCGATCTTCAGttttt; and shBysl-976 Bottom, catgaaaaaCTGAAGATCGCAGAAATGGAAggacagcacacTTCCATCTCTACGATCCTCAGc. Each pair of oligonucleotides consists of the 21-nucleotide sense strand of the target (first set of capital letters) with three G-T mismatch mutations (underlined), the optimized loop sequence derived from the human microRNA (lowercase letters), the antisense strand (second set of capital letters), the RNA polymerase III transcription terminator, and the overhanging sequences (37).

For the *Bysl* episomal expression vectors, the full-length mouse *Bysl* cDNA (GenBank accession number AK143027; 1,308 bp) was amplified by RT-PCR from blastocyst RNA and cloned into pHPCAG or pPPCAG in which the PGK-hph-pA cassette in pHPCAG was replaced by the PGK-pac-pA cassette. For the Bysl-Venus fusion constructs, Venus (39) was fused to the C terminus of Bysl by the linker peptide RSESLVNSAVDGTAGPGST derived from pEGFP-N1 (Clontech).

The RNAi-resistant Bysl-Venus construct was obtained by introducing silent mutations that do not change the coded amino acid sequence into *Bysl-Venus* cDNA using inverse PCR. Three silent mutations were generated in each sequence complementary to shBysl-845 and shBysl-976. The wild-type coding region in the pHPCAG or pPPCAG expression vector was replaced by the mutated sequence. The deletion mutants of Bysl fused to Venus were also constructed using inverse PCR.

For the expression of Bysl-Venus in embryos, the *EGFP* cDNA in the pcDNA3.1EGFP-poly(A83) vector (70) was replaced by the cDNA encoding Bysl-Venus. After linearization of the expression vector, in vitro mRNA transcription was performed using the RiboMAX Large Scale RNA Production Systems-T7 kit (Promega) in the presence of $m^7G(5')ppp(5')G$ RNA capping

analog (Invitrogen). A few picoliters of 100 ng/μl denatured mRNA was microinjected.

ES cell culture and supertransfection. MGZ5 ES cells (44) were cultured in the absence of feeder cells in Dulbecco's modified Eagle medium supplemented with 15% fetal calf serum, 1 mM sodium pyruvate, 0.1 mM 2-mercaptoethanol, 0.1 mM nonessential amino acids, 50 U/ml penicillin-streptomycin, 1,000 U/ml of leukemia inhibitory factor (LIF), 100 μg/ml G418, and 10 μg/ml zeocin on gelatin-coated dishes. For supertransfection with episomal vectors, MGZ5 ES cells, which had been plated the previous day at a density of 3×10^4 cells/well in 24-well plates, were transfected with 1 to 4 μg/ml supercoiled plasmid vectors using Lipofectamine 2000 (Invitrogen) in 300 μl of Opti-MEM I containing 10% fetal calf serum for 3 to 4 h and then replated into six-well plates. One day after transfection, the cells were selected with 1 μg/ml puromycin or 100 μg/ml hygromycin B. Six to seven days after transfection, the cells were fixed and stained for alkaline phosphatase (AP) activity.

Pulse-chase labeling of rRNA. Metabolic labeling of rRNA was performed as previously described (59). At 48 h posttransfection, ES cells were preincubated in methionine-free medium for 15 min and then incubated in medium containing 50 μCi/ml L-[*methyl*-^{3}H]methionine (Amersham Biosciences) for 30 min. The cells were subsequently chased with nonradioactive medium containing 15 μg/ml L-methionine for various time periods. Following pulse-chase labeling, RNA was isolated using Sepasol RNA I Super reagent. Label incorporation was measured by scintillation counting, and samples containing equal amounts of radioactivity were electrophoresed on a 1% agarose-formaldehyde gel and transferred to a nylon membrane (GeneScreen Plus; PerkinElmer), which was sprayed with En^{3}Hance (PerkinElmer) and exposed to Kodak BioMax MS film at −80°C for 3 days.

Sucrose density gradient fractionation. Polysome profiles were analyzed as previously described (59). At 48 h posttransfection, ES cells were treated with 50 μg/ml cycloheximide (CHX) for 10 min and harvested by trypsinization. Equal numbers of cells from each sample were resuspended in lysis buffer (20 mM Tris-HCl [pH 7.4], 130 mM KCl, 10 mM $MgCl_2$, 2.5 mM dithiothreitol, 0.5% NP-40, 0.5% sodium deoxycholate, 10 μg/ml CHX, 0.2 mg/ml heparin, and 200 U/ml RNase inhibitor [TOYOBO]) and incubated on ice for 15 min. The lysates were centrifuged at 15,000 × *g* for 15 min and the supernatants were layered over 10 to 45% (wt/wt) sucrose density gradients in polysome buffer (10 mM Tris-HCl [pH 7.4], 60 mM KCl, 10 mM $MgCl_2$, 1 mM dithiothreitol, 0.1 mg/ml heparin) formed with Biocomp Gradient Master. The gradients were centrifuged at 220,000 × *g* for 30 min or at 160,000 × *g* for 100 min at 4°C in an RPS55T-2 rotor (Hitachi) and fractionated using a BIOCOMP piston gradient fractionator equipped with a Bio-Mini UV monitor for continuous measurement of the absorbance at 260 nm.

Transmission electron microscopy. Preimplantation embryos microinjected with siRNAs were exposed to acidic Tyrode's solution (Sigma) for removal of the zona pellucida and fixed with 2.5% glutaraldehyde in 0.1 M phosphate buffer (pH 7.0) at 4°C overnight. The embryos were washed, postfixed in 1% osmium tetroxide for 60 min on ice, dehydrated with a series of ethanol gradients, and embedded in Epon 812 resin mixture (TAAB). The resin was polymerized at 70°C for 2 days. Ultrathin sections were stained with 2% uranyl acetate in 70% ethanol and Raynold's lead citrate and examined on a Hitachi H-7500 electron microscope.

RESULTS

***Bysl* is crucial for the development of preimplantation embryos.** In an attempt to elucidate the molecular mechanisms underlying developmental processes of preimplantation embryos, we identified several genes that are highly expressed in preimplantation embryos by in silico analysis. We selected 89 such genes whose functions have not been fully characterized and analyzed their expression patterns by RT-PCR. Of 77 genes detected in preimplantation embryos, we picked 32 genes that were preferentially expressed in embryos compared to in adult tissues. To investigate possible roles in preimplantation development, we screened these genes by using siRNA. A mixture of two distinct siRNA duplexes for each gene was microinjected into the cytoplasm of fertilized eggs at E0.5. In this screen, five genes were identified as factors whose depletion by siRNA inhibited blastocyst development. Among these genes, the development of embryos injected with siRNA against *Bysl* was most significantly impaired just prior to blastocyst formation, suggesting direct involvement of *Bysl* in this process.

Microarray analyses have shown that *Bysl* is enriched in embryonic stem cells and certain types of adult stem cells (hematopoietic, neural, and retinal stem/progenitor cells) in mice (18, 25, 26, 49, 63) and humans (1). We found that *Bysl* is highly expressed in preimplantation embryos as well as some adult tissues, including brain, bone marrow, and gonads (Fig. 1A). During the preimplantation stage, *Bysl* mRNA was detected continuously from unfertilized eggs to blastocysts (Fig. 1B), suggesting that *Bysl* is expressed maternally.

Although RNAi is a process of sequence-specific gene silencing, off-target effects can be encountered. To ensure the specificity of RNAi, we performed independent experiments with three distinct siRNAs targeted to different regions of *Bysl* coding sequence. Each *Bysl* siRNA exerted similar phenotypic effects with various efficiencies (Fig. 1C); the severity of the phenotype was correlated with the observed reduction in *Bysl* mRNA levels (Fig. 1D). We used a mixture of highly effective siRNAs (siBysl-845 and siBysl-976) for further analyses, both of which inhibited blastocyst formation in a dose-dependent manner (see Fig. S1 in the supplemental material), thus assuring that the minimum effective amount of siRNA was used. Moreover, the siRNA-dependent developmental arrest could be overcome by coinjecting in vitro synthesized *Bysl* mRNA (Fig. 1E), indicating the specificity of the RNAi effect.

The development of embryos injected with *Bysl* siRNAs was arrested at the 16-cell stage. To determine the time point at which development was arrested, morphological alterations in the *Bysl* siRNA-injected embryos were examined during preimplantation development. When *Bysl* siRNAs were injected into fertilized eggs, compaction at the eight-cell stage occurred normally in vitro. However, blastocyst formation was completely inhibited, although intracellular fluid accumulation in some embryos was observed (Fig. 2A). These embryos failed to hatch from the zona pellucida, could not outgrow in culture even when the zona was removed, and eventually degenerated (all injected embryos). *Oct3/4* siRNA, which was used as a control, also inhibited blastocyst development albeit with a lower efficiency than *Bysl* siRNAs (22% ± 15% developmental rate compared with 96% ± 8% for *EGFP* siRNA). Chronological analysis of the number of nuclei visualized with Hoechst 33342 showed that most of the embryos injected with *Bysl* siRNAs were arrested at the 16-cell stage (Fig. 2B). This was accompanied by reduced BrdU incorporation into newly synthesized DNA (Fig. 2C), while no increase in apoptosis, as determined by terminal deoxynucleotidyltransferase-mediated dUTP nick end labeling assay, was detected up to this stage (data not shown). However, prolonged arrest over 24 h at the 16-cell stage (3.7 days after E0.5 [E0.5+3.7]) inevitably caused embryonic lethality. The developmental arrest at this stage was also observed when siRNAs were injected into both blastomeres of two-cell stage embryos at E1.5 (see Fig. S2 in the supplemental material), suggesting temporal specificity of the requirement for Bysl.

Embryos injected with *Bysl* siRNAs failed to induce differentiation into trophectoderm. Blastocyst formation requires development of the TE layer with concomitant apical-basolat-

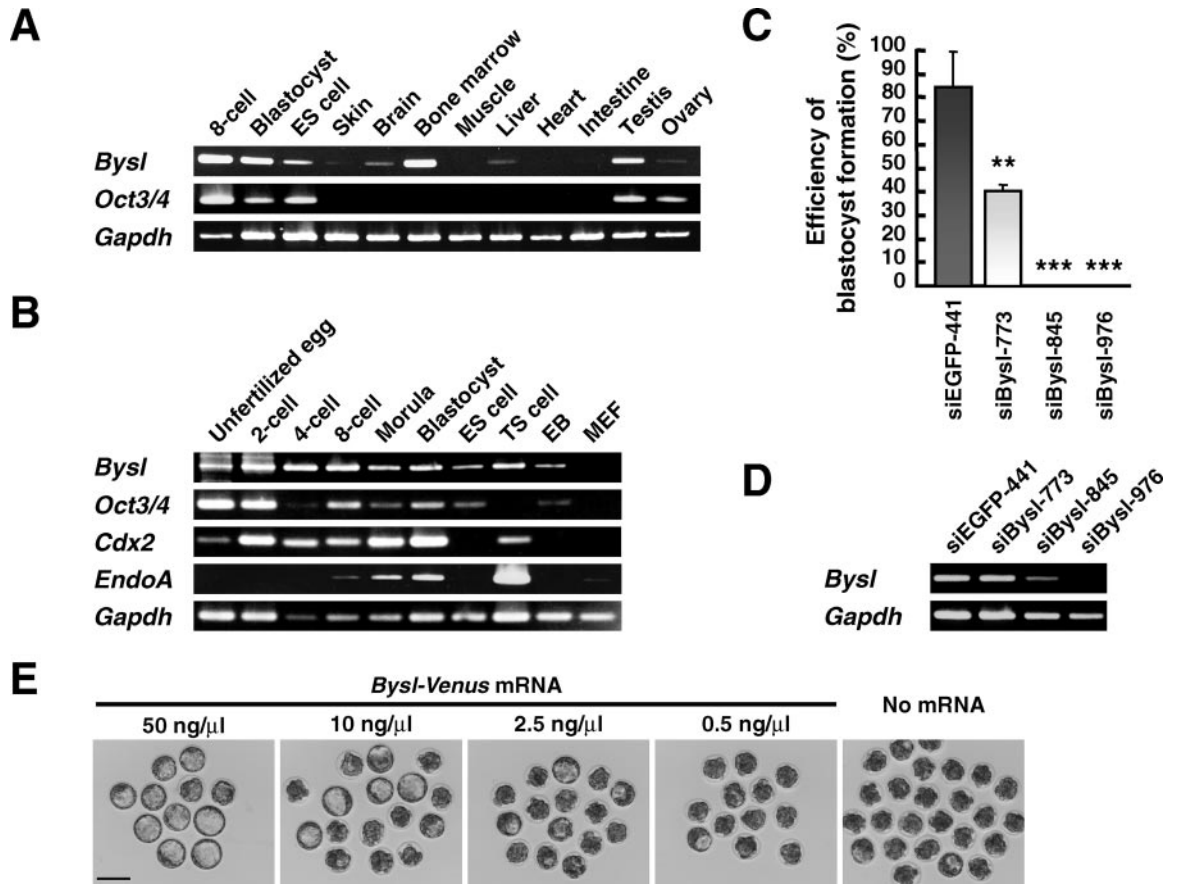

FIG. 1. *Bysl* is crucial for the development of preimplantation embryos. (A) *Bysl* expression in various mouse tissues was analyzed by RT-PCR. *Oct3/4* is a marker for pluripotent and germ line cells. (B) *Bysl* expression during the preimplantation period. *Oct3/4* expression was restricted to pluripotent stem cells, while *Cdx2* and *EndoA* were specifically expressed in the trophoblast lineage. TS, trophoblast stem; EB, embryoid body 10 days after plating; MEF, mouse embryonic fibroblast. (C) Three distinct siRNAs against *Bysl* inhibited blastocyst formation. Fertilized eggs were microinjected with 20 μM siRNA solution at E0.5, and blastocyst formation was evaluated four days after injection (E0.5+4.0). Each value represents the mean ± standard deviation from three independent experiments. Total numbers of embryos injected with siEGFP-441, siBysl-773, siBysl-845, and siBysl-976 were 40, 46, 54, and 51, respectively. Significance levels were determined by Student's *t* test (**, $P < 0.01$; ***, $P < 0.001$). (D) The severity of the phenotype was correlated with the effective downregulation of *Bysl* mRNA. *Bysl* expression was analyzed by RT-PCR at E0.5+3.25. (E) Developmental arrest caused by *Bysl* siRNAs was overcome by coinjecting *Bysl* mRNA in a dose-dependent manner. Embryos were injected with a mixture containing 5 μM each of siBysl-845 and siBysl-976 and various concentrations of in vitro synthesized *Bysl-Venus* mRNA used in the experiment whose results are described in Fig. 4B. The embryos were photographed at E0.5+4.0. Scale bar, 100 μm.

eral membrane polarity which allows vectorial fluid secretion and a tight junctional permeability seal that facilitates fluid accumulation (57). Therefore, we determined whether differentiation into TE was induced in *Bysl* siRNA-injected embryos. RT-PCR analysis of the injected embryos showed that the expression of the cytokeratin *EndoA* gene, an early TE marker, was slightly reduced (Fig. 2D). The failure to induce TE-specific gene expression was corroborated by immunostaining. Control blastocysts showed assembled EndoA structures in the TE layer (Fig. 2E, upper panels). In contrast, no such organized structures were detected in the *Bysl* siRNA-injected embryos (Fig. 2E, lower panels). We also examined the expression of Oct3/4 and Cdx2, the two mutually antagonistic and lineage-specific transcription factors that are involved in segregation of the pluriblast and trophoblast lineages, respectively (41, 44, 60). Oct3/4 was detectable in both inner and outer cells of control morulae and early blastocysts (Fig. 2F, upper and middle panels, respectively). On the other hand, Cdx2 was repressed in the inner cells as early as the morula stage but was maintained in the outer cells at the morula stage through the blastocyst stage, consistent with a previous report (44). In the *Bysl* siRNA-injected embryos (Fig. 2F, lower panels), however, Cdx2 was barely detectable, whereas Oct3/4 was maintained at the equivalent stage. These results indicate that the nascent differentiation toward the TE lineage is abolished by the silencing of *Bysl*.

Episomal expression of *Bysl* shRNAs inhibited proliferation of embryonic stem cells. Next, we investigated the function of *Bysl* in ES cells, because the expression and functional requirement for *Bysl* in the epiblast, the embryonic counterpart of ES cells, have been shown (5). To achieve stable and homogeneous expression of siRNA in ES cells, we constructed a polyoma-based episomal RNAi vector harboring the human U6 promoter for shRNA expression. Using episomal supertransfection (19), we found that expression of both shBysl-845 and shBysl-976 markedly inhibited proliferation of ES cells

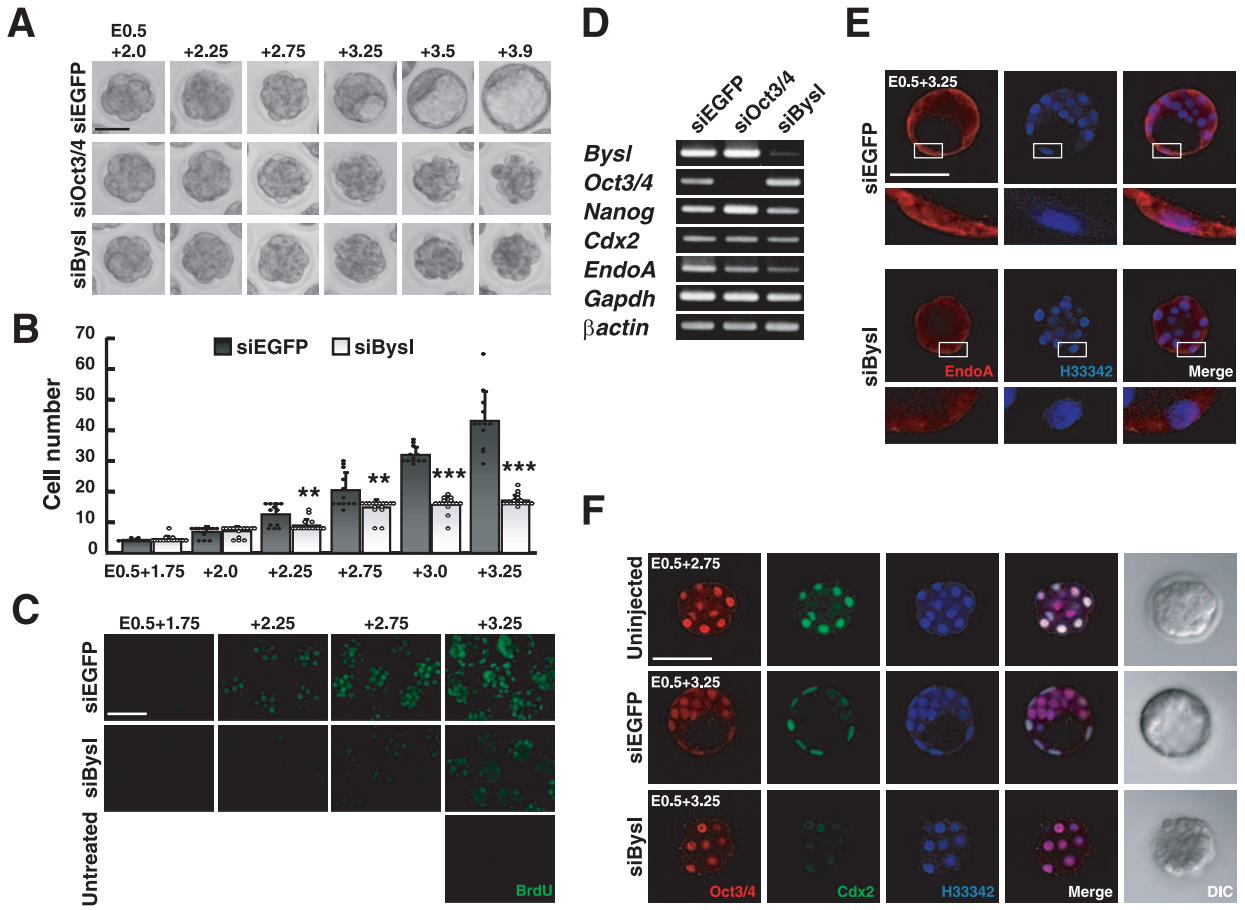

FIG. 2. The development of embryos injected with *Bysl* siRNAs was arrested at the 16-cell stage, resulting in a defect in differentiation toward trophectoderm. (A) Morphological alterations in siRNA-injected embryos were examined during blastocyst formation. Embryos were injected with 20 μM siEGFP-441, siOct3/4-670, or siBysl mixture containing 10 μM each of siBysl-845 and siBysl-976. Scale bar, 50 μm. (B) Cell numbers were determined periodically. Embryos were exposed to 10 μg/ml Hoechst 33342 and squashed under a coverslip, and the numbers of fluorescent nuclei were counted. Similar results were obtained in three independent experiments. **, $P < 0.01$; ***, $P < 0.001$. (C) The proliferative activity was assayed by BrdU incorporation. Untreated, without treatment with BrdU. Scale bar, 100 μm. (D) Marker gene expression was analyzed by RT-PCR at E0.5+3.25. (E) Confocal immunofluorescence imaging of cytokeratin EndoA with TROMA-1 antibody. Nuclei were stained with Hoechst 33342 (H33342). Fourfold-magnified views of the boxed areas are shown in the smaller, lower panels. Scale bar, 50 μm. (F) Immunofluorescent localization of Oct3/4 and Cdx2. Overlapping expression of Oct3/4 and Cdx2 in the nuclei appears white in the merged images. Scale bar, 50 μm. DIC, differential interference contrast.

(Fig. 3A). Fluorescence-activated cell sorting analysis showed no significant differences in cell cycle distribution 48 h post-transfection (see Fig. S3 in the supplemental material). *Bysl* shRNA-treated ES cells exhibited no obvious morphological differentiation, although they appeared to be disorganized (Fig. 3B). Expression of undifferentiated ES cell markers such as *Oct3/4*, *Nanog*, and *Rex1*, or differentiation markers such as *Cdx2*, *Hnf4*α, and *brachyury*, was not altered (Fig. 3C). Moreover, inhibition of proliferation caused by *Bysl* shRNAs was also observed in differentiated ES cells after LIF withdrawal (data not shown), indicating that *Bysl* is required not only for the proliferation of undifferentiated stem cells but also for differentiated cells. Similar results were obtained when another ES cell line, ZHBTc4, was transiently transduced with *Bysl* siRNAs or shRNAs (data not shown).

Bysl localized to the nucleus and was concentrated in the nucleolus. In a previous report, immunocytochemical analysis showed that human BYSL is localized in the cytoplasm of trophoblast cells (62). To analyze the subcellular localization of mouse Bysl, we produced Bysl-Venus by fusing the yellow fluorescent protein Venus to the C terminus of Bysl. Exogenously expressed Bysl-Venus was highly enriched in the nucleolus and was also present diffusely in the nucleoplasm of COS-7 cells, whereas no significant signal was detected in the cytoplasm (Fig. 4A). We obtained a similar localization pattern using Bysl-DsRed fusion protein (see Fig. S4 in the supplemental material). The nucleolar/nucleoplasmic localization of Bysl-Venus was also observed not only in embryos (Fig. 4B) and undifferentiated ES cells (Fig. 4C, upper panels) but also in ES cells differentiated into the trophoblast lineage (Fig. 4C, lower panels).

RNAi-resistant Bysl, which localizes to the nucleolus/nucleoplasm, overcame the proliferation inhibition caused by *Bysl* shRNAs. We next determined whether Bysl-Venus could functionally substitute for endogenous Bysl. For this, an RNAi-resistant *Bysl-Venus* construct was produced by introducing

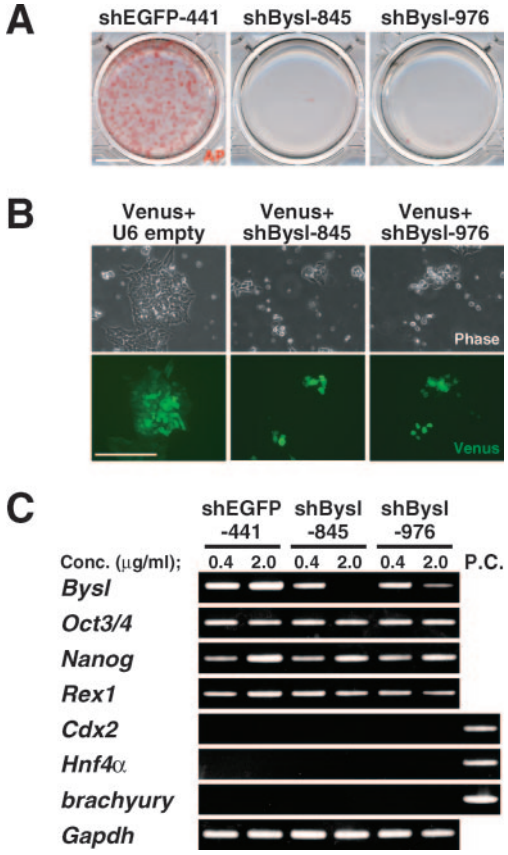

FIG. 3. Episomal expression of *Bysl* shRNAs inhibited proliferation of embryonic stem cells. (A) MGZ5 ES cells were transfected with 2 μg/ml of the pPPU6 episomal shRNA expression vector. One day following transfection, the cells were selected with 1 μg/ml puromycin. Seven days after transfection, undifferentiated ES cell colonies were visualized by staining for AP activity. Scale bar, 10 mm. (B) Morphological alterations in ES cells cotransfected with 1 μg/ml pHPCAG-Venus and 2 μg/ml pPPU6-shRNA. The cells were selected with 1 μg/ml puromycin and 100 μg/ml hygromycin B, and then photographed under epifluorescence at three days posttransfection. Scale bar, 200 μm. (C) Marker gene expression was analyzed by RT-PCR at 48 h posttransfection. *Cdx2*, *Hnf4*α, and *brachyury* are markers for trophoblast, endoderm, and mesoderm differentiation, respectively. ZHBTc4 ES cells (43) cultured in the presence of 1 μg/ml tetracycline for 24 h, MGZ5 ES cells cultured in the absence of LIF for six days, and embryoid bodies five days after plating were used as positive controls (P.C.) for *Cdx2*, *Hnf4*α, and *brachyury*, respectively.

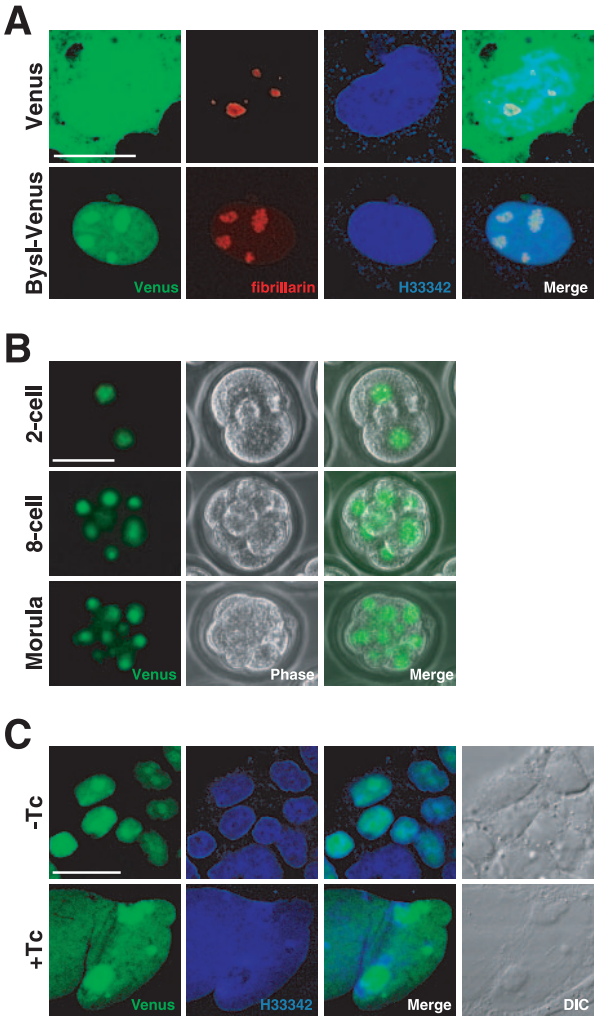

FIG. 4. Bysl localized to the nucleus and was concentrated in the nucleolus. (A) A Bysl-Venus fusion protein was expressed in COS-7 cells. The cells were fixed at one day posttransfection, immunostained for the nucleolar marker fibrillarin, and observed under a confocal laser scanning microscope. Venus alone diffusely distributed throughout the cytoplasm and nucleus (upper panels). H33342, Hoechst 33342. Scale bar, 20 μm. (B) *Bysl-Venus* mRNA transcribed in vitro was injected into fertilized eggs and photographed under epifluorescence one day later (upper panels), or injected into both blastomeres of two-cell stage embryos and photographed one day (middle panels) or two days (lower panels) later. Scale bar, 50 μm. (C) ZHBTc4 ES cells were transfected with a Bysl-Venus construct and cultured in the absence (undifferentiated; upper panels) or presence (differentiated into trophoblast lineage; lower panels) of 1 μg/ml tetracycline (Tc) for four days. Scale bar, 20 μm. DIC, differential interference contrast.

silent mutations into each of the two shRNA target sequences (Fig. 5A and B). Using this construct, we tested whether the expression of RNAi-resistant Bysl-Venus could restore the proliferation of *Bysl* shRNA-treated ES cells. Cotransfection of *Bysl* shRNA and wild-type or silently mutated *Bysl-Venus* expression vectors demonstrated that the mutated *Bysl-Venus* was sufficiently resistant to *Bysl* shRNAs (Fig. 5C). ES cells were first transfected with wild-type or RNAi-resistant *Bysl-Venus* vector and subsequently transduced with *Bysl* shRNAs. Wild-type *Bysl-Venus* partially rescued colony formation in the *Bysl* shRNA-treated ES cells, although the number and size of the colonies were significantly reduced compared to those of the *EGFP* shRNA-treated colonies (Fig. 5D, middle panels). In contrast, the expression of RNAi-resistant *Bysl-Venus* nearly overcame the proliferation inhibition caused by depletion of endogenous *Bysl* (Fig. 5D, lower panels). Taken together, these findings provide evidence that the inhibitory effect is solely due to the silencing of *Bysl* and that Bysl-Venus, which predominantly localizes to the nucleolus/nucleoplasm, can functionally substitute for endogenous Bysl.

Deletion mutants of Bysl, which retain nucleolar localization, exerted a dominant negative effect. Bysl is highly conserved throughout evolution but does not contain any conserved functional domains or nuclear localization motifs. To

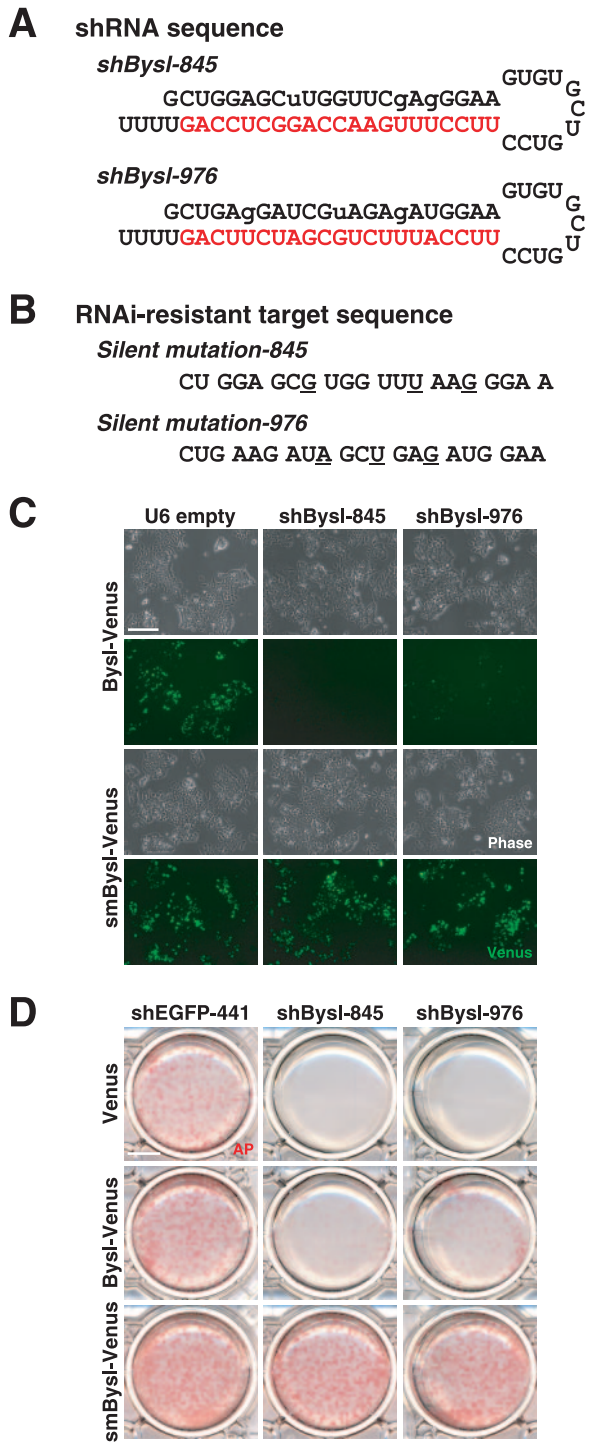

FIG. 5. RNAi-resistant Bysl, which localizes to the nucleolus/nucleoplasm, overcame the proliferation inhibition caused by *Bysl* shRNAs. (A) The predicted structures of two shRNAs against *Bysl*. The three G-U mismatch mutations in the sense strand are presented in lowercase letters. (B) Silent mutations (underlined) were generated within each of the shRNA target sequences in *Bysl-Venus* to confer RNAi resistance. (C) MGZ5 ES cells were cotransfected with shRNA (2 μg/ml) and wild-type or silently mutated (sm) Bysl-Venus (2 μg/ml) expression vectors. The cells were photographed under epifluorescence at two days posttransfection. Note that smBysl-Venus was resistant to *Bysl* shRNAs. Scale bar, 200 μm. (D) Rescue of the knockdown phenotype by expression of RNAi-resistant Bysl. MGZ5 ES cells were first transfected with 2 μg/ml pHPCAG-ByslVenus or -smByslVenus followed by selection with 100 μg/ml hygromycin B. Four days after transfection, equal numbers of cells from each sample were subsequently transfected with 4 μg/ml pPPU6-shRNA followed by selection with 100 μg/ml hygromycin B and 1 μg/ml puromycin. The cells were stained for AP activity six days after the second transfection. Scale bar, 10 mm.

identify the regions critical for its nuclear localization and functionality, deletion mutants were generated (Fig. 6A). The deleted regions share various degrees of amino acid identity/similarity among mice, humans, and yeast. By Western blot analysis, the Bysl-Venus deletion mutants were detected at the predicted molecular sizes, except the d1 (with amino acids 1 through 133 deleted [Δ1-133]) mutant, which was slightly smaller than expected (Fig. 6B). The subcellular localizations of these mutants were altered to various extents compared to that of wild-type Bysl (Fig. 6C). Only d1 and d2 (Δ134-175) retained nucleolar localization, though both were detected in minimal amounts in the nucleoplasm, and d2 displayed a nuclear speckle-like pattern as well. The other three mutants, d3 (Δ176-236), d4 (Δ237-309), and d5 (Δ310-436), accumulated in the cytoplasm and were excluded from the nucleus.

To determine whether the deletion mutants could functionally substitute for endogenous Bysl, ES cells were serially transfected with the *Bysl-Venus* mutant and *Bysl* shRNA expression vectors. None of the mutants were able to rescue the knockdown phenotype in ES cells (Fig. 6D), indicating that all of them are nonfunctional. In addition, d1 and d2, which retain nucleolar localization, suppressed proliferation when overexpressed (Fig. 6E), suggesting that they exerted a dominant negative effect. The close correlation between nucleolar localization of the mutant molecules and their inhibitory effects (Fig. 6F) reinforces the idea that endogenous Bysl functions not in the cytoplasm but in the nucleolus.

***Bysl* is required for 40S ribosome biogenesis.** To investigate the molecular function of Bysl, we examined the involvement of Bysl in ribosome biogenesis because functional Bysl is localized in the nucleolus (Fig. 4 to 6) and yeast Enp1 is involved in pre-rRNA processing and 40S subunit biogenesis (11). The nucleolus is a subnuclear structure that functions primarily in processes of ribosome biogenesis, including rRNA transcription, pre-rRNA processing, and ribosome subunit assembly (45). First, pre-rRNA processing was analyzed by pulse-chase labeling after treatment with *Bysl* shRNAs. Pre-rRNA was pulse-labeled with [*methyl*-^{3}H]methionine at 48 h posttransfection and its processing to mature rRNA was analyzed at various time intervals after chase. During rRNA processing, the primary 47S transcript is rapidly processed to the 20S and 32S intermediates, which are further processed to the mature 18S and 5.8/28S rRNAs, which are components of the 40S and 60S ribosomal subunits, respectively (9, 15, 32). In the *Bysl* shRNA-treated ES cells, the synthesis of the 28S rRNA was not affected. In contrast, the production of the 18S rRNA was greatly inhibited and a marked accumulation of the 20S precursor was observed (15 to 60 min after chase) (Fig. 7A).

Next, the ribosomal profile of cytoplasmic lysates was analyzed by sucrose density gradient sedimentation. The *Bysl* shRNA-treated ES cells showed a dramatic decrease in the

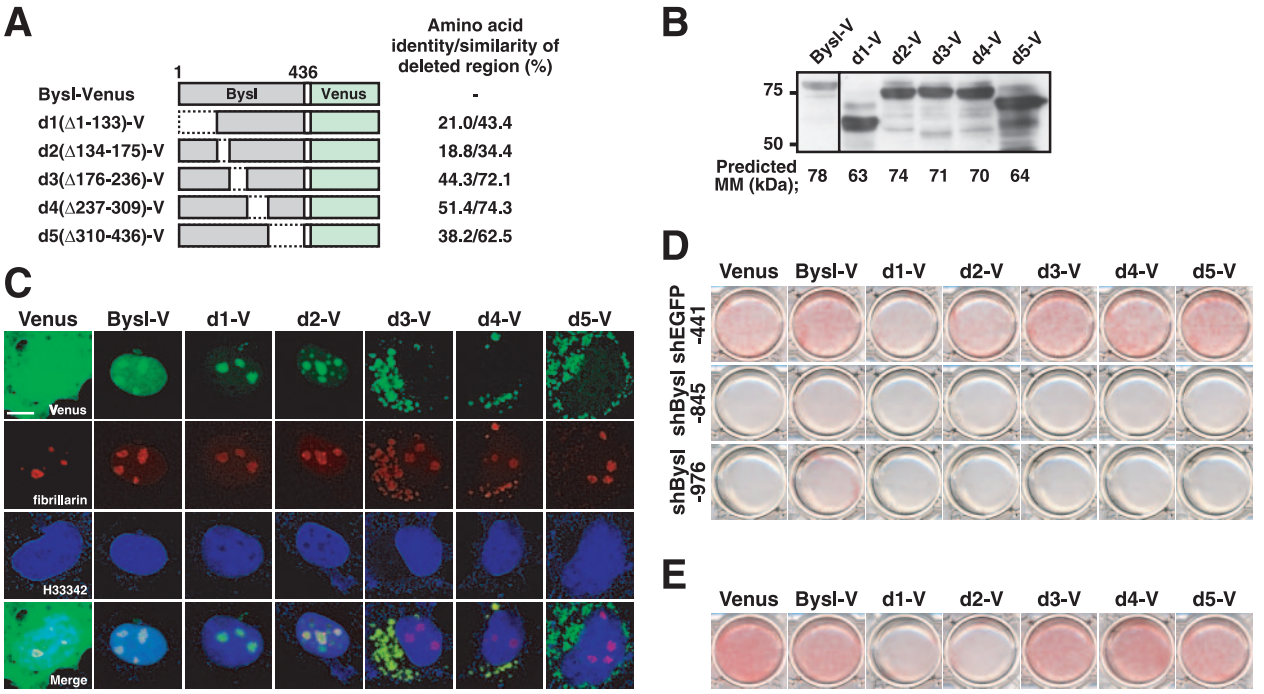

F

	Amino acid identity/similarity of deleted region (%)	Subcellular localization (FIG. 6C)	Rescue of knockdown phenotype (FIG. 6D)	Suppression of proliferation (FIG. 6E)	Dominant negative phenotype (FIG. 7C)
Bysl-Venus	-	No>Np	+	-	-
d1(Δ1-133)-V	21.0/43.4	No>>Np	-	+	+
d2(Δ134-175)-V	18.8/34.4	No/NuSp>>Np	-	+	+
d3(Δ176-236)-V	44.3/72.1	Cy	-	-	ND
d4(Δ237-309)-V	51.4/74.3	Cy	-	-	ND
d5(Δ310-436)-V	38.2/62.5	Cy	-	-	ND

FIG. 6. Deletion mutants of Bysl, which retain nucleolar localization, exerted a dominant negative effect. (A) Schematic representation of Bysl deletion mutants fused to Venus. Deletion mutants were generated based on the sequence similarity among humans, mice, and yeast (32.5% and 54.7% amino acid identity and similarity in total). (B) Western blot analysis of the mutant proteins expressed in COS-7 cells using anti-GFP fluorescent protein antibody (SC-8334; Santa Cruz Biotechnology). The deletion mutants were detected at the predicted molecular masses (MM), except the d1 mutant, which had an observed MM of 55 to 60 kDa. (C) Subcellular localizations of the mutants were determined in COS-7 cells. Note that d1 and d2 retained nucleolar localization. Scale bar, 10 μm. H33342, Hoechst 33342. (D) Functionalities of the deletion mutants were assessed by rescue of the knockdown phenotype in MGZ5 ES cells as described in the legend to Fig. 5D. (E) MGZ5 ES cells were transfected with 2 μg/ml pPPCAG constructs expressing the mutant proteins followed by selection with 1 μg/ml puromycin. The cells were stained for AP activity at six days posttransfection. Note that overexpression of d1 or d2 suppressed the proliferation of ES cells. (F) Summary of the properties of Bysl deletion mutants. The exact relationship between nucleolar localization and inhibitory effect is noted. Cy, cytoplasm; Np, nucleoplasm; No, nucleolus; NuSp, nuclear speckle-like; ND, not determined.

quantity of free 40S subunits, resulting in an accumulation of 60S subunits: the 40S/60S ratios of cells treated with shBysl-845 and shBysl-976 were 14% and 22% of control, respectively (Fig. 7B, left panels). Polysomal mRNAs that are actively engaged in translation were also decreased (Fig. 7B, right panels). Overexpression of deletion mutant d1 or d2 also provoked a decrease in cytoplasmic 40S ribosomal subunits (the 40S/60S ratio was 40% of control for both mutants) (Fig. 7C), which can be attributed to the dominant negative effect. Taken together, these results demonstrate that Bysl plays a crucial role in the maturation of pre-40S ribosomal particles through involvement in 18S rRNA processing.

Finally, we determined whether *Bysl* siRNA-injected embryos exhibit any defects in ribosome biogenesis by using transmission electron microscopy. In mice, embryonic nucleologenesis, in which an inactive nucleolus precursor body (NPB) is gradually organized into a functional nucleolus, occurs during preimplantation development (17). At the early cleavage stage, the NPB, seen as an electron-dense fibrillar sphere, is composed of a dense network of uniformly packed filaments. At the onset of rRNA transcription in two- to four-cell stage embryos, a reticulated structure, the nucleolonema, is formed at the periphery of the NPB. Extensive reticulation of the NPB periphery takes place in the four- to eight-cell stage, while the fibrillar sphere remains in the core of the nucleolus until the morula stage (21). Active transcription was detected in the peripheral regions preceded by the assembly of the nucleolar components therein (7, 13, 71), whereas the fibrillar spheres take no part in transcription (30).

In control morulae (around the 16-cell stage), fully differ-

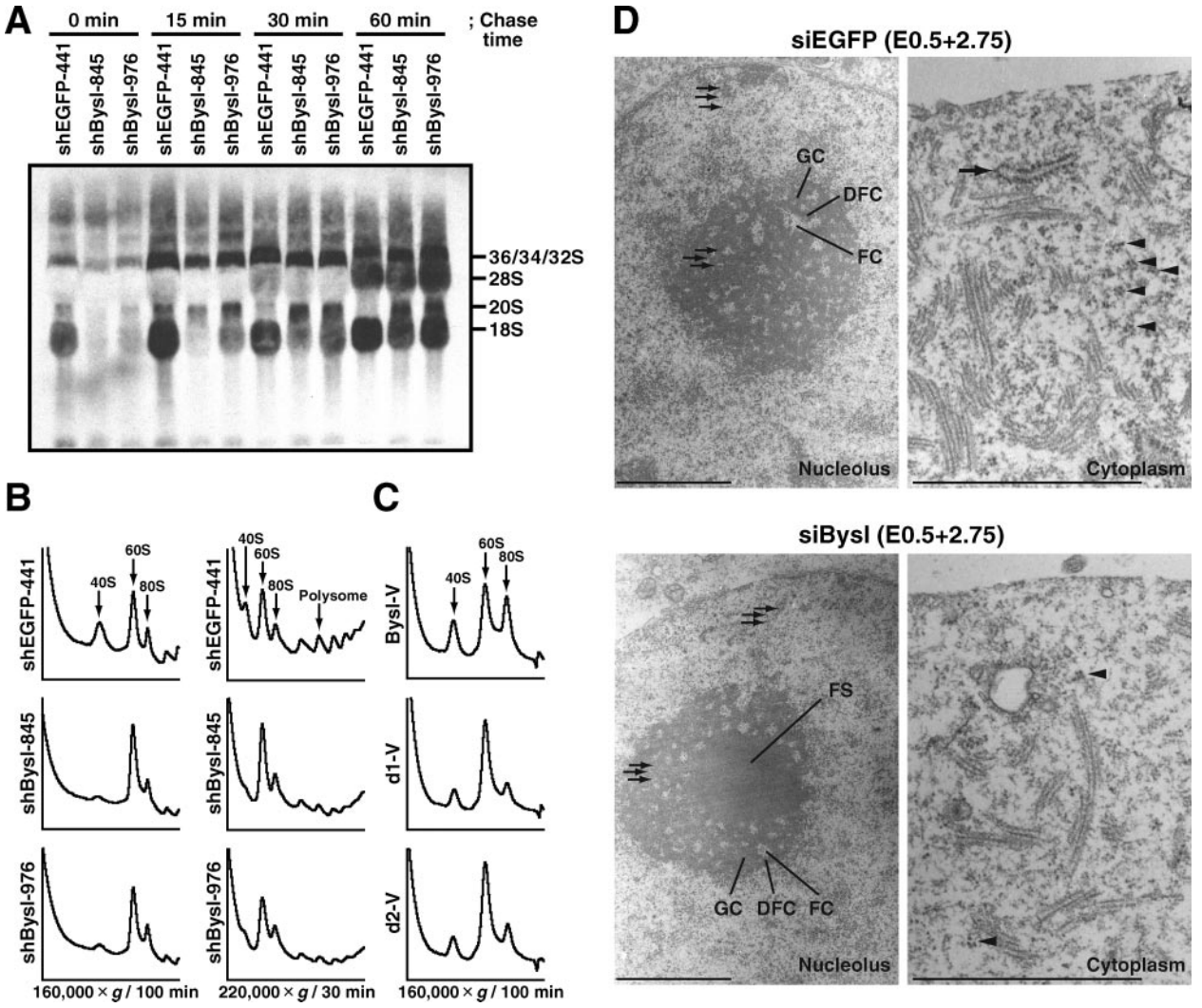

FIG. 7. *Bysl* is required for 40S ribosome biogenesis. (A) Inhibition of rRNA processing in *Bysl* shRNA-treated ES cells. MGZ5 ES cells, which had been plated the previous day at a density of 6×10^4 cells/well in 12-well plates, were transfected with 2 μg/ml pPPU6-shRNA followed by selection with 1 μg/ml puromycin. At 48 h posttransfection, the cells were pulse-labeled with L-[*methyl*-^{3}H]methionine for 30 min and subsequently chased in nonradioactive medium for the indicated time. The expected positions of mature rRNAs and major precursors are indicated on the right. Similar results were obtained in three independent experiments. (B and C) A deficit in 40S ribosomal subunits in ES cells transfected with *Bysl* shRNA (B) or deletion mutant (C) expression vectors. At 48 h posttransfection, cytoplasmic extracts from 1.0×10^6 (B) or 1.5×10^6 (C) cells per sample were isolated and centrifuged on 10 to 45% sucrose density gradients at 160,000 × *g* for 100 min (B, left panel, and C) or at 220,000 × *g* for 30 min (B, right panel). Absorbancy at 260 nm was continuously monitored. Similar results were obtained in three independent experiments. (D) Impairment of nucleologenesis and ribosome biogenesis in *Bysl* siRNA-injected embryos. Embryos injected with siRNAs were fixed at the 16-cell stage (E0.5+2.75) and examined by transmission electron microscopy. The control embryos contained fully differentiated, reticulated nucleoli composed of FCs surrounded by DFCs and GCs. In contrast, the *Bysl* siRNA-injected embryos contained immature nucleoli in which inactive electron-dense fibrillar spheres (FSs) were apparent at the core. Moreover, in spite of the comparable amounts of preribosomal particles (arrows in left panels) at the nucleolar periphery as well as in the nucleoplasm, only few clustered ribosomes (arrowheads) and rough endoplasmic reticula (arrows in right panel) were observed in the cytoplasm, compared with the control embryos. Scale bar, 1 μm.

entiated, reticulated nucleoli were apparent, and they showed three morphologically distinct nucleolar subcompartments: fibrillar centers (FCs), spherical electron-lucent structures; dense fibrillar components (DFCs), more-electron-dense materials surrounding FCs; and granular components (GCs), in which FC-DFC complexes are embedded (Fig. 7D, upper left panel) (14). These control nucleoli exhibited a substantial number of relatively small FCs, reflecting active transcription (24). The GCs, which are distributed throughout the nucleolus, contained a large quantity of preribosomal particles. It is likely that most of such preribosomal particles in the nucleolus represent precursors of the large subunits because the small ribosomal subunits mature more rapidly than large subunits and are immediately exported to the cytoplasm (22, 48, 65). In contrast, the nucleolar structures remained rudimentary in *Bysl* siRNA-injected embryos. Solid fibrillar spheres were apparent in the cores of the nucleoli, while reticulated structures at the periphery contained several FCs (Fig. 7D, lower left panel). Condensed chromatin was scarcely observed in the nucleoplasm. Furthermore, in spite of the comparable quantities of

preribosomal particles at the nucleolar periphery as well as in the nucleoplasm, clustered ribosomes and rough endoplasmic reticula were inconspicuous in the cytoplasm (Fig. 7D, lower right panel). In conclusion, these data demonstrate that Bysl is crucial for early embryonic development as an integral factor for ribosome biogenesis.

DISCUSSION

In this study, we showed that mouse Bysl is an essential factor for 40S ribosome biogenesis and is crucial for the development of preimplantation embryos as well as the proliferation of ES cells. The development of embryos injected with *Bysl* siRNAs was arrested around the 16-cell stage, and no functional TE was formed. Knockdown of *Bysl* using an episomal shRNA expression vector inhibited proliferation of ES cells. Exogenously expressed Bysl fused to a fluorescent protein exclusively localized to the nucleus with enrichment in the nucleolus. Furthermore, silencing of *Bysl* caused defects in 40S ribosome biogenesis in both ES cells and embryos. These findings suggest that mouse Bysl, like its homologs in lower eukaryotes, plays a crucial role in ribosome biogenesis.

In a previous study using a human trophoblast cell line, BYSL was detected in the cytoplasm by immunocytochemical analysis (62). However, other studies using HeLa cells reported detection of BYSL within purified nucleoli through several independent proteomic analyses (3, 4, 55). In line with the latter reports, we found that both mouse and human Bysl fused to a fluorescent protein localized to the nucleolus/nucleoplasm, whereas no significant fluorescence was detected in the cytoplasm (Fig. 4; see Fig. S5A in the supplemental material). The rescue of RNAi phenotypes in mouse ES cells by ectopic expression of mouse or human Bysl-Venus (Fig. 5D; see Fig. S5E in the supplemental material) indicates that these fusion proteins can functionally substitute for endogenous Bysl. These results show that the cellular compartment in which Bysl executes its function is the nucleolus and/or nucleoplasm but not the cytoplasm.

Deletion mutant analyses further demonstrated the correlation between the nucleolar localization and functional activity of Bysl. *Bysl* is conserved throughout evolution, with higher conservation in the C-terminal half (11, 51). The deletion mutants were generated based on sequence similarity. Among them, d1 and d2, which localized to the nucleolus, exerted a dominant negative effect; in contrast, the other three mutants, which accumulated in the cytoplasm, had no such activity (Fig. 6 and 7C). Therefore, the more conserved middle-to-C-terminal region, but not the N-terminal region, is important for nuclear localization, although the N terminus is required for appropriate function. The involvement of several regions of the protein in its nuclear localization suggests that the presence of intrinsic nuclear localization signals alone is not sufficient. On the other hand, the nucleolar accumulation of human BYSL is dependent upon rRNA transcription in HeLa cells (3), suggesting that the nucleolar targeting is mediated by a variety of molecular interactions with other components of preribosomal ribonucleoprotein particles. In fact, a mutant lacking a putative nucleolar localization signal (35, 68) at residues 37 to 40 (Δ34-40) distributed similarly to the wild-type Bysl (see Fig. S6 in the supplemental material).

Disruption of *Bysl* function using RNAi or dominant negative mutants resulted in lethality with defective ribosome biogenesis in both embryos and ES cells. Pulse-chase labeling of rRNA showed that processing of the 20S precursor to the mature 18S was impaired after *Bysl* silencing, while the synthesis of 28S rRNA was not affected. Ribosomal profiles demonstrated that free 40S subunits were greatly reduced in the cytoplasm. Studies of yeast have shown that ribosomal biogenesis in the nucleolus requires many *trans*-acting factors, such as components of small nucleolar ribonucleoprotein particles, rRNA-modifying enzymes, endo- and exonucleases, RNA helicases, GTP/ATPases, chaperones, and others (reviewed in reference 16). These factors are assembled with rRNAs and ribosomal proteins into a large ribonucleoprotein complex and act to coordinate pre-rRNA processing and ribosomal subunit assembly. The impairment of 18S rRNA processing caused by *Bysl* depletion suggests a direct involvement of Bysl in this step. However, such a phenotype may stem from a defect in the assembly of pre-40S particles as well, because ribosome assembly and pre-rRNA processing are intimately linked (reviewed in reference 67). We found that a small amount of mature 18S rRNA was still processed even when cytoplasmic 40S subunits were nearly depleted. Therefore, these results suggested that *Bysl* is involved in the processing of 18S rRNA, the assembly of 40S preribosomal particles, or both.

Enp1, the yeast homolog of Bysl, is associated with early 90S preribosomes that contain 35S primary transcripts, subsequent pre-40S particles in the nucleolus, and later pre-40S subunits in the cytoplasm but not with mature 40S ribosomal subunits (23, 53, 54). The temperature-sensitive mutant of *ENP1* exhibits defects in 18S rRNA synthesis and nuclear export of pre-40S subunits (11, 54). The results obtained with yeast are consistent with our results with mice except for the following two points. A small percentage of Enp1 is distributed in the cytoplasm (11, 23, 54), while Bysl localizes exclusively to the nucleus (Fig. 4). In addition, the synthesis of 20S pre-rRNA, as well as 18S rRNA, was significantly inhibited in the *enp1* mutants (11) but not in the *Bysl* knockdown cells (Fig. 7A). The former point may be explained by a difference in the compartment where processing of the 20S pre-rRNA to the mature 18S rRNA takes place (9, 52, 65). Bysl may dissociate from the pre-40S in the nucleus after completion of this process, while Enp1 dissociates in the cytoplasm as previously reported (53). The reason for the latter difference is unclear, but it may reflect general differences in processing mechanisms between yeast and mammals (15). The inability of human BYSL, which can substitute for mouse Bysl, to complement the yeast *enp1* mutant (11) also suggests functional differences between these molecules.

Our data show that Bysl is required for blastocyst formation. The development of embryos injected with *Bysl* siRNAs was uniformly arrested around the 16-cell stage, resulting in a failure to induce differentiation into TE. The requirement for Bysl at this stage appears to be temporally specific as injection of embryos with *Bysl* siRNAs at the one-cell stage (E0.5) or the two-cell stage (E1.5) resulted in developmental arrest at the same stage (Fig. 2B; see Fig. S2 in the supplemental material). As *Bysl*-deficient mice die shortly after implantation (5), these results suggest that although zygotic transcription of *Bysl* is dispensable for preimplantation development in the presence of maternal transcripts, their zygotic translation is required for

blastocyst formation. Nevertheless, we could not exclude the possibility that Bysl is also required before blastocyst formation, due to the possible persistence of maternal protein. The developmental arrest just prior to the blastocyst stage may reflect the maternal-to-zygotic transition in the translation machinery and the increased need for protein synthesis during blastocyst formation. The resumption of rRNA transcription is first detected at the two-cell stage in parallel with the major transcriptional activation of the zygotic genome, and rRNA synthesis gradually increases thereafter (12, 21, 71). The rate of ribosomal protein synthesis (31), along with the number of ribosomes (47), rises sharply after the eight-cell stage, followed by increased rates of protein synthesis at the blastocyst stage (10). In addition, unlike for compaction, which seems to be regulated by posttranslational mechanisms (34), virtually concomitant protein synthesis is required for blastocyst cavitation (29), suggesting that certain types or amounts of proteins crucial for blastocyst formation are immediately translated prior to this process. Depletion of *Bysl* should lead to a deficit in zygotic ribosomes and a failure to initiate zygotic translation, which in turn would affect the protein synthesis important for cell division and differentiation. In fact, the expression of *EndoA* and *Cdx2* at the mRNA level was slightly or not obviously affected by the silencing of *Bysl*, but their protein expression levels were significantly reduced (Fig. 2). In line with these results, a number of mice carrying loss-of-function mutations in factors involved in ribosome biogenesis die at the preimplantation stage prior to blastocyst formation, including ribosomal protein Rps19 (36), rRNA processing factors, such as fibrillarin (40) and pescadillo (33), and other nonribosomal factors, such as Aatf (also called Traube) (64). Among these proteins, the yeast homologs of fibrillarin and Aatf, Nop1 and Bfr2, respectively, have been reported to associate with Enp1 (20).

We identified *Bysl* as a preimplantation embryo- and stem cell-associated gene by in silico analysis. *Bysl* is highly expressed in embryonic stem cells and certain types of adult stem cells, showing a decrease in expression with a loss of differentiation capacity (18, 25, 26, 49, 63). Global gene expression profiles derived from large-scale cDNA sequencing showed that *Bysl* is expressed not only in embryos including pre- and postimplantation stages but also in fetal tissues and some types of adult tissues, suggesting that *Bysl* plays an important role in a broader spectrum of cells. In fact, no significant change in *Bysl* mRNA levels was observed in ES cells after differentiation was induced by LIF withdrawal or forced repression of Oct3/4, at least for a short period (data not shown). We also detected high levels of *Bysl* mRNA in several tumor cell lines and found that the silencing of *Bysl* affected proliferation of B16-F10 melanoma cells (data not shown). From these observations, the expression of *Bysl* appears to be simply coupled with rapid cell proliferation but not with the differentiation state. With regard to the regulation of *Bysl* expression, systematic approaches using microarray analyses identified the human *BYSL* as a major transcriptional target of c-MYC based on gene expression correlation, and direct binding of MYC to the 5′ untranslated region of the *BYSL* gene, which contains a canonical E-box element (5′-CACGTG-3′), was demonstrated by a chromatin immunoprecipitation assay (8, 56). As Myc is required for proliferation and morphogenetic differentiation in preimplantation embryos (46) and is critical for the maintenance of pluripotency and self-renewal in ES cells (2), these observations suggest that Bysl is a critical downstream effector of Myc in the regulation of ribosome biogenesis.

In this report, we have shown that mouse *Bysl* is a conserved essential factor for ribosome biogenesis in eukaryotes and is localized in the nucleus. The discrepancy with the previous study showing that human BYSL mediated cell adhesion in vitro and was detected in the cytoplasm by immunocytochemical analysis (62) may be explained by the fact that the cDNA for BYSL used in that report was partial. The expression assays for cell adhesion activity and protein interaction in vitro and the hybridoma screening for the identification of a monoclonal antibody against BYSL were performed using the partial cDNA. Actually, the monoclonal antibody was shown to detect a specific band at 35 kDa (62), although endogenous BYSL has a molecular mass of approximately 50 kDa (55), indicating that this antibody recognizes a protein different from the full-length BYSL. The reason why cell adhesion mediated by TRO was enhanced by expression of a partial *BYSL* cDNA is not clear since we demonstrated that the Bysl deletion mutant d1 (Δ1-133), which corresponds to the partial form of BYSL, acts as a dominant negative mutant (Fig. 6). Nevertheless, given that a partial BYSL protein has any functional significance, its enhancing effect on cell adhesion may be a secondary consequence of global translational regulation or other extraribosomal mechanisms. Because the plasma membrane protein TRO is also localized to the nuclear envelope and could target BYSL to the nuclear envelope (6), BYSL expression may regulate the distribution or activity of TRO, which in turn would affect cell adhesion. It is noted, however, that *Tro*-deficient ES cells do not show any morphological or proliferative abnormalities (38), indicating that the essential role of Bysl described here is independent of Tro-mediated cell adhesion.

Our conclusion that mammalian Bysl plays a crucial role in 40S ribosomal subunit biogenesis is consistent with the role of yeast Enp1. Despite the fact that the fundamental mechanism that underlies ribosome biogenesis is conserved between yeast and mammals, the detailed strategies are distinctly different. In comparison with that in yeast, however, the regulation of ribosome biogenesis in mammals is largely unknown. In this regard, the identification of Bysl as a critical component of 40S subunit synthesis provides informative insights into the molecular mechanisms governing mammalian ribosome biogenesis.

ACKNOWLEDGMENTS

We are grateful to H. Niwa (CDB, RIKEN, Japan) for the MGZ5 and ZHBTc4 ES cells, pHPCAG episomal expression vector, and rabbit anti-Oct3/4 antiserum. We thank M. N. Fukuda (The Burnham Institute, CA) for antibodies against BYSL and valuable discussion, A. Miyawaki (Brain Science Institute, RIKEN, Japan) for the Venus coding sequence, K. Yamagata (University of Tsukuba, Japan) for pcDNA3.1-poly(A) vector, S. Tanaka (University of Tokyo, Japan) for trophoblast stem cells, and Y. Watanabe (University of Tokyo, Japan) for technical instructions for ribosomal profiling. We also thank S. Kakuta, D. C. Lee, S. Takashima, and H. Okae for helpful discussions and comments. The TROMA-1 antibody, developed by P. Brulet and R. Kemler, was obtained from the Developmental Studies Hybridoma Bank developed under the auspices of the NICHD and maintained by The University of Iowa, Department of Biological Sciences, Iowa City, IA.

This research was supported by Grants-in-Aid from the Ministry of Education, Culture, Sports, Science and Technology of Japan, and a fellowship from the Japan Society for the Promotion of Science.

REFERENCES

1. **Abeyta, M. J., A. T. Clark, R. T. Rodriguez, M. S. Bodnar, R. A. Pera, and M. T. Firpo.** 2004. Unique gene expression signatures of independently-derived human embryonic stem cell lines. Hum. Mol. Genet. **13:**601–608.
2. **Adhikary, S., and M. Eilers.** 2005. Transcriptional regulation and transformation by Myc proteins. Nat. Rev. Mol. Cell Biol. **6:**635–645.
3. **Andersen, J. S., Y. W. Lam, A. K. Leung, S. E. Ong, C. E. Lyon, A. I. Lamond, and M. Mann.** 2005. Nucleolar proteome dynamics. Nature **433:**77–83.
4. **Andersen, J. S., C. E. Lyon, A. H. Fox, A. K. Leung, Y. W. Lam, H. Steen, M. Mann, and A. I. Lamond.** 2002. Directed proteomic analysis of the human nucleolus. Curr. Biol. **12:**1–11.
5. **Aoki, R., N. Suzuki, B. C. Paria, K. Sugihara, T. O. Akama, G. Raab, M. Miyoshi, D. Nadano, and M. N. Fukuda.** 2006. The Bysl gene product, bystin, is essential for survival of mouse embryos. FEBS Lett. **580:**6062–6068.
6. **Aoyama, J., Y. Nakayama, D. Sugiyama, S. Saburi, D. Nadano, M. N. Fukuda, and N. Yamaguchi.** 2005. Apical cell adhesion molecule, trophinin, localizes to the nuclear envelope. FEBS Lett. **579:**6326–6332.
7. **Baran, V., J. Vesela, P. Rehak, J. Koppel, and J. E. Flechon.** 1995. Localization of fibrillarin and nucleolin in nucleoli of mouse preimplantation embryos. Mol. Reprod. Dev. **40:**305–310.
8. **Basso, K., A. A. Margolin, G. Stolovitzky, U. Klein, R. Dalla-Favera, and A. Califano.** 2005. Reverse engineering of regulatory networks in human B cells. Nat. Genet. **37:**382–390.
9. **Bowman, L. H., B. Rabin, and D. Schlessinger.** 1981. Multiple ribosomal RNA cleavage pathways in mammalian cells. Nucleic Acids Res. **9:**4951–4966.
10. **Brinster, R. L., J. L. Wiebold, and S. Brunner.** 1976. Protein metabolism in preimplanted mouse ova. Dev. Biol. **51:**215–224.
11. **Chen, W., J. Bucaria, D. A. Band, A. Sutton, and R. Sternglanz.** 2003. Enp1, a yeast protein associated with U3 and U14 snoRNAs, is required for pre-rRNA processing and 40S subunit synthesis. Nucleic Acids Res. **31:**690–699.
12. **Clegg, K. B., and L. Piko.** 1983. Quantitative aspects of RNA synthesis and polyadenylation in 1-cell and 2-cell mouse embryos. J. Embryol. Exp. Morphol **74:**169–182.
13. **Cuadros-Fernández, J. M., and P. Esponda.** 1996. Immunocytochemical localisation of the nucleolar protein fibrillarin and RNA polymerase I during mouse early embryogenesis. Zygote **4:**49–58.
14. **Derenzini, M., M. Thiry, and G. Goessens.** 1990. Ultrastructural cytochemistry of the mammalian cell nucleolus. J. Histochem. Cytochem. **38:**1237–1256.
15. **Eichler, D. C., and N. Craig.** 1994. Processing of eukaryotic ribosomal RNA. Prog. Nucleic Acid Res. Mol. Biol. **49:**197–239.
16. **Fatica, A., and D. Tollervey.** 2002. Making ribosomes. Curr. Opin. Cell Biol. **14:**313–318.
17. **Fléchon, J. E., and V. Kopecný.** 1998. The nature of the "nucleolus precursor body" in early preimplantation embryos: a review of fine-structure cytochemical, immunocytochemical and autoradiographic data related to nucleolar function. Zygote **6:**183–191.
18. **Fortunel, N. O., H. H. Otu, H. H. Ng, J. Chen, X. Mu, T. Chevassut, X. Li, M. Joseph, C. Bailey, J. A. Hatzfeld, A. Hatzfeld, F. Usta, V. B. Vega, P. M. Long, T. A. Libermann, and B. Lim.** 2003. Comment on "'Stemness': transcriptional profiling of embryonic and adult stem cells" and "a stem cell molecular signature." Science **302:**393.
19. **Gassmann, M., G. Donoho, and P. Berg.** 1995. Maintenance of an extrachromosomal plasmid vector in mouse embryonic stem cells. Proc. Natl. Acad. Sci. USA **92:**1292–1296.
20. **Gavin, A. C., M. Bosche, R. Krause, P. Grandi, M. Marzioch, A. Bauer, J. Schultz, J. M. Rick, A. M. Michon, C. M. Cruciat, M. Remor, C. Hofert, M. Schelder, M. Brajenovic, H. Ruffner, A. Merino, K. Klein, M. Hudak, D. Dickson, T. Rudi, V. Gnau, A. Bauch, S. Bastuck, B. Huhse, C. Leutwein, M. A. Heurtier, R. R. Copley, A. Edelmann, E. Querfurth, V. Rybin, G. Drewes, M. Raida, T. Bouwmeester, P. Bork, B. Seraphin, B. Kuster, G. Neubauer, and G. Superti-Furga.** 2002. Functional organization of the yeast proteome by systematic analysis of protein complexes. Nature **415:**141–147.
21. **Geuskens, M., and H. Alexandre.** 1984. Ultrastructural and autoradiographic studies of nucleolar development and rDNA transcription in preimplantation mouse embryos. Cell Differ. **14:**125–134.
22. **Gleizes, P. E., J. Noaillac-Depeyre, I. Leger-Silvestre, F. Teulieres, J. Y. Dauxois, D. Pommet, M. C. Azum-Gelade, and N. Gas.** 2001. Ultrastructural localization of rRNA shows defective nuclear export of preribosomes in mutants of the Nup82p complex. J. Cell Biol. **155:**923–936.
23. **Grandi, P., V. Rybin, J. Bassler, E. Petfalski, D. Strauss, M. Marzioch, T. Schafer, B. Kuster, H. Tschochner, D. Tollervey, A. C. Gavin, and E. Hurt.** 2002. 90S pre-ribosomes include the 35S pre-rRNA, the U3 snoRNP, and 40S subunit processing factors but predominantly lack 60S synthesis factors. Mol. Cell **10:**105–115.
24. **Haaf, T., D. L. Hayman, and M. Schmid.** 1991. Quantitative determination of rDNA transcription units in vertebrate cells. Exp. Cell Res. **193:**78–86.
25. **Hüttmann, A., U. Duhrsen, K. Heydarian, L. Klein-Hitpass, T. Boes, A. W. Boyd, and C. L. Li.** 2006. Gene expression profiles in murine hematopoietic stem cells revisited: analysis of cDNA libraries reveals high levels of translational and metabolic activities. Stem Cells **24:**1719–1727.
26. **Ivanova, N. B., J. T. Dimos, C. Schaniel, J. A. Hackney, K. A. Moore, and I. R. Lemischka.** 2002. A stem cell molecular signature. Science **298:**601–604.
27. **Johnson, M. H., and C. A. Ziomek.** 1981. The foundation of two distinct cell lineages within the mouse morula. Cell **24:**71–80.
28. **Kamath, R. S., A. G. Fraser, Y. Dong, G. Poulin, R. Durbin, M. Gotta, A. Kanapin, N. Le Bot, S. Moreno, M. Sohrmann, D. P. Welchman, P. Zipperlen, and J. Ahringer.** 2003. Systematic functional analysis of the Caenorhabditis elegans genome using RNAi. Nature **421:**231–237.
29. **Kidder, G. M., and J. R. McLachlin.** 1985. Timing of transcription and protein synthesis underlying morphogenesis in preimplantation mouse embryos. Dev. Biol. **112:**265–275.
30. **Kopecný, V., V. Landa, and A. Pavlok.** 1995. Localization of nucleic acids in the nucleoli of oocytes and early embryos of mouse and hamster: an autoradiographic study. Mol. Reprod. Dev. **41:**449–458.
31. **LaMarca, M. J., and P. M. Wassarman.** 1979. Program of early development in the mammal: changes in absolute rates of synthesis of ribosomal proteins during oogenesis and early embryogenesis in the mouse. Dev. Biol. **73:**103–119.
32. **Lapik, Y. R., C. J. Fernandes, L. F. Lau, and D. G. Pestov.** 2004. Physical and functional interaction between Pes1 and Bop1 in mammalian ribosome biogenesis. Mol. Cell **15:**17–29.
33. **Lerch-Gaggl, A., J. Haque, J. Li, G. Ning, P. Traktman, and S. A. Duncan.** 2002. Pescadillo is essential for nucleolar assembly, ribosome biogenesis, and mammalian cell proliferation. J. Biol. Chem. **277:**45347–45355.
34. **Levy, J. B., M. H. Johnson, H. Goodall, and B. Maro.** 1986. The timing of compaction: control of a major developmental transition in mouse early embryogenesis. J. Embryol. Exp. Morphol. **95:**213–237.
35. **Lohrum, M. A., M. Ashcroft, M. H. Kubbutat, and K. H. Vousden.** 2000. Identification of a cryptic nucleolar-localization signal in MDM2. Nat. Cell Biol. **2:**179–181.
36. **Matsson, H., E. J. Davey, N. Draptchinskaia, I. Hamaguchi, A. Ooka, P. Leveen, E. Forsberg, S. Karlsson, and N. Dahl.** 2004. Targeted disruption of the ribosomal protein S19 gene is lethal prior to implantation. Mol. Cell. Biol. **24:**4032–4037.
37. **Miyagishi, M., H. Sumimoto, H. Miyoshi, Y. Kawakami, and K. Taira.** 2004. Optimization of an siRNA-expression system with an improved hairpin and its significant suppressive effects in mammalian cells. J. Gene Med. **6:**715–723.
38. **Nadano, D., K. Sugihara, B. C. Paria, S. Saburi, N. G. Copeland, D. J. Gilbert, N. A. Jenkins, J. Nakayama, and M. N. Fukuda.** 2002. Significant differences between mouse and human trophinins are revealed by their expression patterns and targeted disruption of mouse trophinin gene. Biol. Reprod. **66:**313–321.
39. **Nagai, T., K. Ibata, E. S. Park, M. Kubota, K. Mikoshiba, and A. Miyawaki.** 2002. A variant of yellow fluorescent protein with fast and efficient maturation for cell-biological applications. Nat. Biotechnol. **20:**87–90.
40. **Newton, K., E. Petfalski, D. Tollervey, and J. F. Caceres.** 2003. Fibrillarin is essential for early development and required for accumulation of an intron-encoded small nucleolar RNA in the mouse. Mol. Cell. Biol. **23:**8519–8527.
41. **Nichols, J., B. Zevnik, K. Anastassiadis, H. Niwa, D. Klewe-Nebenius, I. Chambers, H. Scholer, and A. Smith.** 1998. Formation of pluripotent stem cells in the mammalian embryo depends on the POU transcription factor Oct4. Cell **95:**379–391.
42. **Niwa, H., T. Burdon, I. Chambers, and A. Smith.** 1998. Self-renewal of pluripotent embryonic stem cells is mediated via activation of STAT3. Genes Dev. **12:**2048–2060.
43. **Niwa, H., J. Miyazaki, and A. G. Smith.** 2000. Quantitative expression of Oct-3/4 defines differentiation, dedifferentiation or self-renewal of ES cells. Nat. Genet. **24:**372–376.
44. **Niwa, H., Y. Toyooka, D. Shimosato, D. Strumpf, K. Takahashi, R. Yagi, and J. Rossant.** 2005. Interaction between Oct3/4 and Cdx2 determines trophectoderm differentiation. Cell **123:**917–929.
45. **Olson, M. O., K. Hingorani, and A. Szebeni.** 2002. Conventional and nonconventional roles of the nucleolus. Int. Rev. Cytol. **219:**199–266.
46. **Paria, B. C., S. K. Dey, and G. K. Andrews.** 1992. Antisense c-myc effects on preimplantation mouse embryo development. Proc. Natl. Acad. Sci. USA **89:**10051–10055.
47. **Pikó, L., and K. B. Clegg.** 1982. Quantitative changes in total RNA, total poly(A), and ribosomes in early mouse embryos. Dev. Biol. **89:**362–378.
48. **Puvion-Dutilleul, F., J. P. Bachellerie, and E. Puvion.** 1991. Nucleolar organization of HeLa cells as studied by in situ hybridization. Chromosoma **100:**395–409.
49. **Ramalho-Santos, M., S. Yoon, Y. Matsuzaki, R. C. Mulligan, and D. A. Melton.** 2002. "Stemness": transcriptional profiling of embryonic and adult stem cells. Science **298:**597–600.
50. Reference deleted.
51. **Roos, J., J. M. Luz, S. Centoducati, R. Sternglanz, and W. J. Lennarz.** 1997.

ENP1, an essential gene encoding a nuclear protein that is highly conserved from yeast to humans. Gene **185:**137–146.
52. **Rouquette, J., V. Choesmel, and P. E. Gleizes.** 2005. Nuclear export and cytoplasmic processing of precursors to the 40S ribosomal subunits in mammalian cells. EMBO J. **24:**2862–2872.
53. **Schäfer, T., B. Maco, E. Petfalski, D. Tollervey, B. Bottcher, U. Aebi, and E. Hurt.** 2006. Hrr25-dependent phosphorylation state regulates organization of the pre-40S subunit. Nature **441:**651–655.
54. **Schäfer, T., D. Strauss, E. Petfalski, D. Tollervey, and E. Hurt.** 2003. The path from nucleolar 90S to cytoplasmic 40S pre-ribosomes. EMBO J. **22:** 1370–1380.
55. **Scherl, A., Y. Coute, C. Deon, A. Calle, K. Kindbeiter, J. C. Sanchez, A. Greco, D. Hochstrasser, and J. J. Diaz.** 2002. Functional proteomic analysis of human nucleolus. Mol. Biol. Cell **13:**4100–4109.
56. **Schlosser, I., M. Holzel, M. Murnseer, H. Burtscher, U. H. Weidle, and D. Eick.** 2003. A role for c-Myc in the regulation of ribosomal RNA processing. Nucleic Acids Res. **31:**6148–6156.
57. **Smith, R., and A. McLaren.** 1977. Factors affecting the time of formation of the mouse blastocoele. J. Embryol. Exp. Morphol. **41:**79–92.
58. **Stewart, M. J., and E. K. Nordquist.** 2005. Drosophila Bys is nuclear and shows dynamic tissue-specific expression during development. Dev. Genes Evol. **215:**97–102.
59. **Strezoska, Z., D. G. Pestov, and L. F. Lau.** 2000. Bop1 is a mouse WD40 repeat nucleolar protein involved in 28S and 5.8S rRNA processing and 60S ribosome biogenesis. Mol. Cell. Biol. **20:**5516–5528.
60. **Strumpf, D., C. A. Mao, Y. Yamanaka, A. Ralston, K. Chawengsaksophak, F. Beck, and J. Rossant.** 2005. Cdx2 is required for correct cell fate specification and differentiation of trophectoderm in the mouse blastocyst. Development **132:**2093–2102.
61. **Suzuki, N., J. Nakayama, I. M. Shih, D. Aoki, S. Nozawa, and M. N. Fukuda.** 1999. Expression of trophinin, tastin, and bystin by trophoblast and endometrial cells in human placenta. Biol. Reprod. **60:**621–627.
62. **Suzuki, N., J. Zara, T. Sato, E. Ong, N. Bakhiet, R. G. Oshima, K. L. Watson, and M. N. Fukuda.** 1998. A cytoplasmic protein, bystin, interacts with trophinin, tastin, and cytokeratin and may be involved in trophinin-mediated cell adhesion between trophoblast and endometrial epithelial cells. Proc. Natl. Acad. Sci. USA **95:**5027–5032.
63. **Tanaka, T. S., T. Kunath, W. L. Kimber, S. A. Jaradat, C. A. Stagg, M. Usuda, T. Yokota, H. Niwa, J. Rossant, and M. S. Ko.** 2002. Gene expression profiling of embryo-derived stem cells reveals candidate genes associated with pluripotency and lineage specificity. Genome Res. **12:**1921–1928.
64. **Thomas, T., A. K. Voss, P. Petrou, and P. Gruss.** 2000. The murine gene, Traube, is essential for the growth of preimplantation embryos. Dev. Biol. **227:**324–342.
65. **Udem, S. A., and J. R. Warner.** 1973. The cytoplasmic maturation of a ribosomal precursor ribonucleic acid in yeast. J. Biol. Chem. **248:**1412–1416.
66. **Ui-Tei, K., Y. Naito, F. Takahashi, T. Haraguchi, H. Ohki-Hamazaki, A. Juni, R. Ueda, and K. Saigo.** 2004. Guidelines for the selection of highly effective siRNA sequences for mammalian and chick RNA interference. Nucleic Acids Res. **32:**936–948.
67. **Warner, J. R.** 1990. The nucleolus and ribosome formation. Curr. Opin. Cell Biol. **2:**521–527.
68. **Weber, J. D., M. L. Kuo, B. Bothner, E. L. DiGiammarino, R. W. Kriwacki, M. F. Roussel, and C. J. Sherr.** 2000. Cooperative signals governing ARF-mdm2 interaction and nucleolar localization of the complex. Mol. Cell. Biol. **20:**2517–2528.
69. **Wianny, F., and M. Zernicka-Goetz.** 2000. Specific interference with gene function by double-stranded RNA in early mouse development. Nat. Cell Biol. **2:**70–75.
70. **Yamagata, K., T. Yamazaki, M. Yamashita, Y. Hara, N. Ogonuki, and A. Ogura.** 2005. Noninvasive visualization of molecular events in the mammalian zygote. Genesis **43:**71–79.
71. **Zatsepina, O., C. Baly, M. Chebrout, and P. Debey.** 2003. The step-wise assembly of a functional nucleolus in preimplantation mouse embryos involves the cajal (coiled) body. Dev. Biol. **253:**66–83.